

# We are IntechOpen, the world's leading publisher of Open Access books Built by scientists, for scientists

6,900

Open access books available

186,000

International authors and editors

200M

Downloads

Our authors are among the

154

Countries delivered to

TOP 1%

most cited scientists

12.2%

Contributors from top 500 universities



WEB OF SCIENCE™

Selection of our books indexed in the Book Citation Index  
in Web of Science™ Core Collection (BKCI)

Interested in publishing with us?  
Contact [book.department@intechopen.com](mailto:book.department@intechopen.com)

Numbers displayed above are based on latest data collected.  
For more information visit [www.intechopen.com](http://www.intechopen.com)



# Assessment of Evapotranspiration in North Fluminense Region, Brazil, Using Modis Products and Sebal Algorithm

José Carlos Mendonça<sup>1</sup>, Elias Fernandes de Sousa<sup>2</sup>,  
Romísio Geraldo Bouhid André<sup>3</sup>, Bernardo Barbosa da Silva<sup>4</sup>  
and Nelson de Jesus Ferreira<sup>5</sup>

<sup>1</sup>*Laboratório de Meteorologia (LAMET/UENF). Rod. Amaral Peixoto,  
Av. Brennand s/n Imboassica, Macaé, RJ*

<sup>2</sup>*Laboratorio de Engenharia Agrícola (LEAG/UENF); Avenida Alberto Lamago,  
CCTA, sl 209, Parque Califórnia, Campos dos Goytacazes, RJ*

<sup>3</sup>*Instituto Nacional de Meteorologia (INMET/MAPA); Eixo Monumental,  
Via S1 – Sudoeste, Brasília, DF*

<sup>4</sup>*Departamento de Ciências Atmosféricas (DCA/UFCG); Avenida  
Aprígio Veloso, Bodocongó, Campina Grande, PB*

<sup>5</sup>*Centro de Previsão de Tempo e Estudos Climáticos (CPTEC/INPE);  
Av. dos Astronautas, Jardim da Granja, São José dos Campos, SP  
Brazil*

## 1. Introduction

North Fluminense Region, Rio de Janeiro State, Brazil (Fig. 1) is known as a sugar cane producer. The production during harvest season 2007/08 were 4 million tons of sugar cane, that were transformed into 4.8 million sacks of sugar, 36,786 liters anhydrous alcohol (ethanol) and 91,008 liters of hydrated alcohol. Economically generated 250 million U. S. dollars (Morgado, 2009). However, this activity is declining in the region due to different factors, including hidric deficit and the use of irrigation techniques may reverse this situation(Azevedo et al., 2002). Some authors (Ide e Oliveira, 1986; Magalhães, 1987) define temperature as a factor of greater importance for sugar cane physiology maturation (ripening) because more the affecting nutrients and water absorption through transpiration flux is a non-controllable condition. Soil humidity is another preponderant factor to sugar cane physiology and varies in function of the cultivation cycle, development stage, climactic conditions and others factors, such as spare water in the soil. The soil moisture content varies during the growth that corresponds to the main cause of production variation. However, the precipitation distribution along the year and spare soil water for the plant disposition are more important in the vegetative cycle of the sugar cane that total precipitation. (Magalhães, 1987).

The physical properties of energy exchange between the plant community and environment such as momentum, latent heat, sensible heat and others are evidenced by the influence they

exert on physiological processes of plants and the occurrence of pests and diseases, which affect the productive potential of plants species exploited economically (Frota, 1978). The radiation components measurements of energy balance in field conditions have direct applicability in agricultural practices, especially in irrigation rational planning, appropriate use of land in regional agricultural zoning, weather variations impact on agricultural crops, protecting plants, among others. The knowledge advance in micro-scale weather, as well as the instrumental monitoring technology evolution has allowed a research increase in this area. Energy balance studies on a natural surface based on energy conservation principle. By accounting means for components that make up this balance, can be evaluate the net radiation plots used for the flow of sensible and latent heat.

The analysis of data collected by artificial satellites orbiting planet earth, allows the determination of various physical properties of planet, consequently, spatial and temporal modifications of different ecosystems are able to be identified.

According Moran et al. (1989), estimative of evapotranspiration - ET, based in data collected in meteorological stations have the limitation of representing punctual values that are capable of satisfactory representing local conditions but, if the objective is to obtain analysis of a regional variation of ET using a method with interpolation and extrapolation from micro-meteorological parameters of an specific area, these punctual data may increase the uncertainty of the analysis.

Trying to reduce such uncertainty degree, different algorithms were developed during the last decades to estimate surface energy flux based in the use of remote sensing techniques.

Bastiaanssen (1995) developed the 'Surface Energy Balance Algorithm for Land - SEBAL', with its validation performed in experimental campaigns in Spain and Egypt (arid climate) using Landsat 5 -TM images. This model involves the spatial variability of the most agro-meteorological variables and can be applied to various ecosystems and requires spatial distributed visible, near-infrared and thermal infrared data together with routine weather data. The algorithm computes net radiation flux -  $R_n$ , sensible heat flux -  $H$  and soil heat flux -  $G$  for every pixel of a satellite image and latent heat flux -  $LE$  is acquired as a residual in energy balance equation (Equation 01). This is accomplished by first computing the surface radiation balance, flowed by the surface energy balance. Although SEBAL has been designed to calculate the energy partition at the regional scale with minimum ground data (Teixeira, 2008).

Roerink et al. (1997) also used Landsat 5 -TM images to evaluate irrigation's performance in Argentina and AVHRR/NOAA sensor images in Pakistan. Combination of Landsat 5 - TM and NOAA/AVHRR images were used by Timmermans and Meijerink (1999) in Africa. Latter, Hafeez et al. (2002) used the SEBAL algorithm with the ASTER sensor installed onboard 'Terra' satellite while studying Pumpanga river region in Philippines. These authors concluded that the combination of the high spatial resolution of ETM+ and ASTER sensors, together with the high temporal resolution from AVHRR and MODIS, provided high precision results of water balance and water use studies on regional scale.

In Brazil, several research center are conducting research using the SEBAL algorithm specially 'Federal University of Campina Grande, PB - UFCG', 'National Institute of Space Research - INPE' and others.

Sebal was developed and validated in arid locations and one of its peculiarities is the use of two anchors pixels (hot pixel -  $LE = 0$  and cold pixel -  $H = 0$ ) with the determination or

selection of hot pixel easier in dry climates. In humid and sub-humid climates is not easy determine a hot pixel, where the latent heat flux is zero or null.

The objectives of the research described in this work are (i) to evaluate two propositions to estimate the sensible heat flux (H) and (ii) to evaluate two methods for conversion of ETinst values to ET24h on the daily evapotranspiration to estimate evapotranspiration in regional scale using SEBAL algorithm, MODIS images, the two propositions to estimate H and meteorological data of the four surface meteorological stations.

## 2. Materials and methods

### 2.1 Study area

The Norte Fluminense region in Rio de Janeiro State, Brazil, has an area of 9.755,1 km<sup>2</sup>, corresponding to 22% of the state's total area. Among its agricultural production, sugar cane plantations are predominant as well as cattle production. In the last years irrigation technologies for fruit production are being promoted and implemented by the government. Nowadays, passion fruit, guava, coconut and pineapple plantations extend for more than 4.000 ha (SEAAPI, 2006).

According Koppen, this region's climate is classified as Aw, that is, tropical humid with rainy summers, dry winters and temperatures average above 18 °C during the coolest months. The annual mean temperatures are of 24°C, with a little thermal amplitude and mean rain precipitation values of 1.023 mm (Gomes, 1999).

The area under study is showed in Figure 1, comparing the area of the Norte Fluminense region within the Rio de Janeiro state and the RJ state within Brazil.



Fig. 1. Study area localization.

### 2.2 Digital orbital images – MODIS images

Daily MOD09 and MYD09 data (Surface Reflectance - GHK / 500 m and GQK / 250 m) and MOD11A1 and MYD11A1 data (Surface Temperature - LST) were used in this research, totalizing 24 scenes over the 'tile' h14/v11 corresponding to Julian Day 218th, 227th, 230th, 241st, 255th, 285th, 320th and 339th in 2005 and 15th, 36th, 63rd, 102nd, 116th, 139th, 166th, 186th, 189th, 190th, 191st, 200th, 201st, 205th, 208th and 221st in 2006. These days were selected because no cloud covering was registered over the study area during the satellite's course over the area were obtained from the Land Processes Distributed Active Archive Center (LP-DAAC), of the National Aeronautics and Space Administration (NASA), at <http://edcimswww.cr.usgs.gov/pub/imswelcome/>.

The GHK – 500 m (Blue, Green, Red, Nir, Mir, Fir, Xir) reflectance band were resampled from 500 m to 250 m. The Red and Nir bands were excluded and GQK (250 m) bands included. This operation aimed to input the value of the red and nir bands in the algorithm. The LST bands were also resampled from 1000 m to 250 m.

The software Erdas Image – Pro, version 8.7 was used for the piles, compositions, clippings and algebra. The Model Maker tool was used to application of the algorithm and the thematic maps were produced using the software ArcGis 9.0.

### 2.3 Meteorological data

Surface data were collected in two micro-meteorological stations from the Universidade Estadual do Norte Fluminense – UENF, installed over agricultural areas cultivated with sugar cane (geographical coordinates:  $21^{\circ} 43' 21,8''$  S and  $41^{\circ} 24' 26,1''$  W), and 'dwarf green' coconut irrigated (geographical coordinates:  $21^{\circ} 48' 31,2''$  S and  $41^{\circ} 10' 46,2''$  W).

The micrometeorological stations installed in both areas (sugar cane and coconut) were equipped with the following sensor: 1 Net radiometer NR Lite (Kipp and Zonen), 2 Piranometer LI 200 (Li-Cor), 2 Probe HMP45C-L (Vaissala), 2 Met One Anemometer (RN Yong) and 3 HFP01SC\_L Soil Heat Flux Plat (Hukseflux). All data from were collected every minute and average values extracted and stores every 15 min in a datalogger CR21X (Sugar cane) and CR 1000 (coconut). Both dataloggers are Campbell Scientific's (USA). The horizontal bars were placed 0.50 m above crop canopy (first level) and 2.0 m between the first and second bars. This standard was maintained all crop cycle and bars relocated where necessary (sugar cane station). In coconut station the relocated was not necessary.

These stations were installed in the center of an area of 5,000 hectare (sugar cane – Santa Cruz Agroindustry) 256 hectare (coconut – Agriculture Taí).



Fig. 2. Localization of the surface micro-meteorological and meteorological stations installed in the study area.

The meteorological stations, both installed on grass (*Paspalum Notatum* L.) are property of research center. The Thies Clima model (Germany) installed at the UENF's Evapotranspiration Station – Pesagro Research Center, (geographical coordinates: 21° 24' 48" S and 41° 44' 48" W) is an automatic station. Is equipped with 1 Anemometer, 1 Barometer, 1 Termohygrometer, 1 Piranometer and 1 Pluviometer. All sensor are connected to a datalogger model DL 12 – V. 2.00 – Thies Clima, recording values every minute and stored an average every 10 minutes.

The Agrosystem model install at the Meteorological Station of the Experimental Campus 'Dr. Leonel Miranda' – UFRRJ, (geographical coordinates: 21° 17' 36" S and 41° 48' 09" W) contains 1 Anemometer, 1 Barometer, 1 Termohygrometer, 1 Piranometer and 1 Pluviometer and recording values every minute and stored an average every 10 minutes.

All geographical coordinates are related to Datum WGS 84 – zone 24, with average altitude of 11 m. The localization of the surface stations, where meteorological data used in this study were collected are showed in Figure 2.

**2.4 Real evapotranspiration estimation with SEBAL**

To calculate surface radiation balance was used the Model Maker tool from the software Erdas Image 8.6. The estimations of the incident solar radiation and the long wave radiation emitted by the atmosphere to the surface were performed in electronic sheet.

To better understand the different phases of the Sebal algorithm using Modis products, a general diagram of the computational routines are shown in Figure 3.

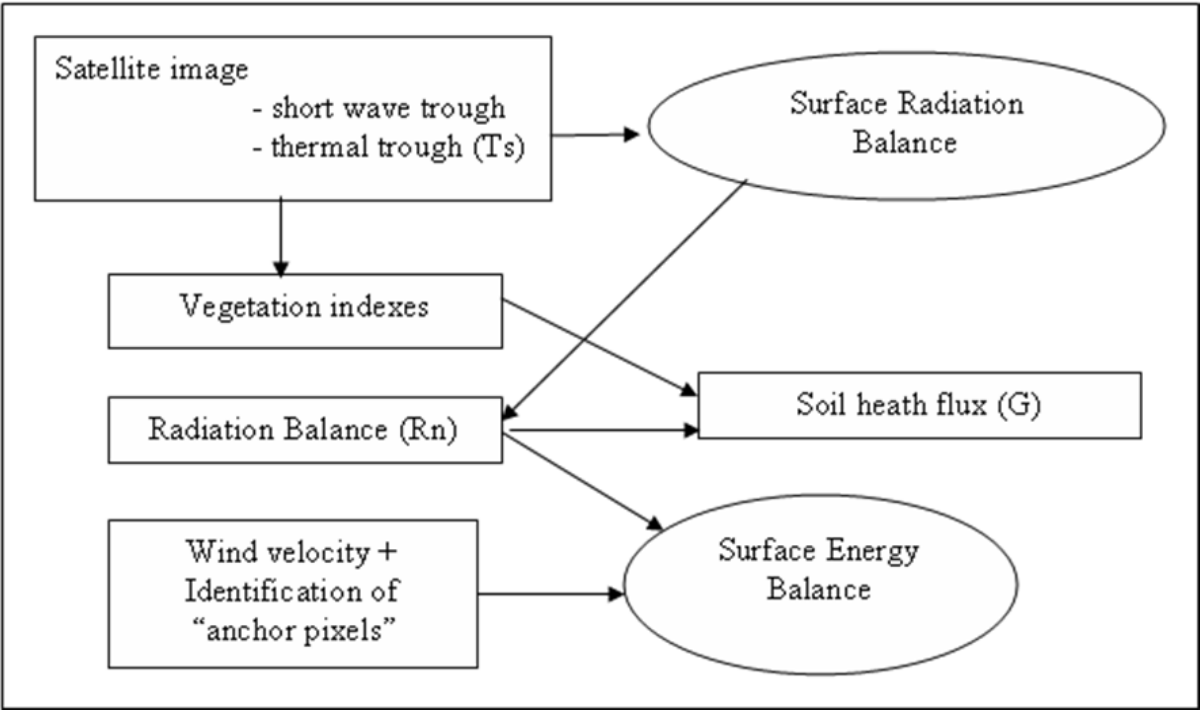


Fig. 3. Diagram of the computational routines for determination of the Surface Energy Balance using SEBAL, form MODIS products. (Modified from Trezza (2002).

A schematic diagram for the estimation of the surface radiation balance (Rn), adapted to MODIS images is showed in Figure 4.

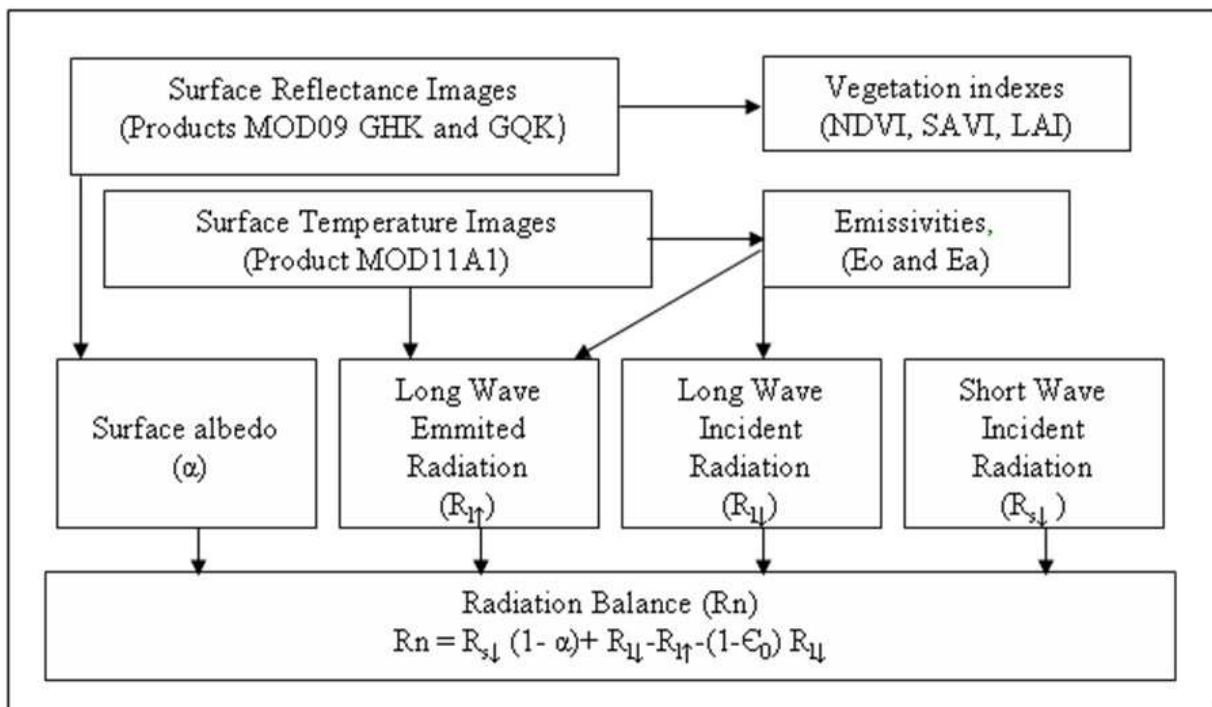


Fig. 4. Diagram showing the process steps of the surface radiation balance adapted for MODIS images.

Detailed processes, as well as the equations for the SEBAL algorithm development, may be obtained in Bastiaanssen et al. (1998). In the present work two propositions were assumed to select the anchor pixels, the first was similar to the one used by Bastiaanssen (1995), with the selection of two pixels with external temperatures (hot pixel/LE = 0 and cool pixel/H = 0). The hot pixel always comprising an area of exposed soil with little vegetation and the cool pixel localized in the interior of a great extension water body. The first proposition was called as 'H\_Classic'.

With the hypothesis that the linear relation  $dT = a + d.T_s$  would be better represented with the selection of a hot pixel with its energy balance components previously known, specially the sensible heat flux (H) and in regions of humid and sub-humid climate be difficult identifying de hot pixels, which can hardly meet the condition of being dry, or have LE = 0, the second hypothesis was formulated. The criterion used for the selection of the cool pixel was the same as in the first hypothesis, that is, to be localized inside a water body of a great extension, but the selection of the hot pixel, where determination of the H values estimate as residue of the Penman-Monteih FAO56 equation using meteorological data from installed at the UENF's Evapotranspiration Station - Pesagro Research Center. This second hypothesis was called 'H\_Pesagro'.

## 2.5 Latent heat flux (LE)

Latent heat flux (vapor transference to the atmosphere trough the process of vegetal transpiration and soil water evaporation) was computed by the simple difference between the radiation balance cards, soil heat flux and sensible heat flux:

$$LE = R_n - G - H \quad (1)$$

where:  $LE$  represents the latent heat flux,  $Rn$  is the radiation balance and  $G$  is the soil heat flux, all expressed in  $W\ m^{-2}$  and obtained during the course of the satellite over the study area.

The value of the instantaneously latent heat flux ( $LE_{inst}$ ), integrated at the time (hour) of the satellites passage ( $mm\ h^{-1}$ ) is:

$$LE_{inst} = 3600 \frac{LE}{\lambda} \quad (2)$$

where:  $LE_{inst}$  is the value of instantaneously ET, expressed in  $mm\ h^{-1}$ ;  $LE$  is the latent heat flux at the moment of the sensor's course and  $\lambda$  is the water vaporization latent heat, expressed by the equation:

$$\lambda = 2,501 - 0,00236 (Ts - 273,16) * 10^6 \quad (3)$$

where:  $Ts$  is the surface temperature chart ( $^{\circ}C$ ) obtained by the product MOD11A1 (K).

With the radiation balance, soil heat flux and latent heat flux charts, the evaporative fraction was obtained and expressed by the equation:

$$\Lambda = \frac{LE}{Rn - G} \quad (4)$$

The evaporative fraction has an important characteristic, it regularity and constancy in clear sky days. In this sense, we can admit that its instantaneously character represents its diurnal mean value satisfactorily, enabling the estimation of daily evapotranspiration by the equation:

$$ET_{24h} = \frac{86400 \Lambda Rn_{24h}}{\lambda} \quad (5)$$

where:  $Rn_{24h}$  is the mean radiation balance occurred during a period of 24 h, expressed in  $W.m^{-2}$ , obtained by the equation:

$$Rn_{24h} = (1 - \alpha) Rs_{24h} - 110 \tau_{sw} 24h \quad (6)$$

where:  $\alpha$ , is the surface albedo;  $Rs_{24h}$  is the daily mean radiation of short incident wave expressed in  $W\ m^{-2}$  and  $\tau_{sw} 24h$ , is the mean daily atmospheric transmissivity.

To determine  $Rs_{24h}$  values, an approximation similar to the method proposed by Lagouarde and Brunet (1983) for the estimation of diurnal cycles of  $Rn$  and  $Rs_{\downarrow}$  in clear sky days, was used. With the values of  $Rn_{24h}$ ,  $Rs_{24h}$  and the surface albedo, extracted from the PESAGRO pixel, a linear regression between these values was performed to obtain a regression equation, its coefficients  $a_1$  and  $b_1$  and then to calculate the  $Rn_{24h}$  chart as a function of the short wave balance. To determine the linear regression the following equation was used:

$$Rn_{24h} = a_1 (1 - \alpha) * Rs_{24h} + b_1 \quad (7)$$

Allen et al. (2002) defined the evaporative fraction of reference (ET<sub>rF</sub>) as the relation between the  $ET_{inst}$  chart and the  $ET_o$  integrated at the same moment and computed with data obtained from a meteorological station, that is:

$$ET_{rF} = \frac{ET_{inst}}{ET_{FAO56}} \quad (8)$$

This procedure generates a type of hourly-culture coefficient ( $k_{c\_h}$ ), admitting that this relation represents the daily relation expressed by the equation:

$$K_{c\_h} = \frac{ET_{inst}}{ET_{oh}} = \frac{ET_{24}}{ET_{o24}} \quad (9)$$

Admitting the relation represented in equation 09 it is possible to obtain the  $ET_{24h}$  expressed in  $\text{mm day}^{-1}$  from the equation:

$$ET_{24h} = ET_{rF} * ET_{o24} \quad (10)$$

In the present work, four values of  $ET_{24h_{SEBAL}}$  were estimated for the same day, applying equations 5 and 10 to the 'H\_Classic' and H\_Pesagro' propositions.

### 3. Results and discussion

#### 3.1 Daily evapotranspiration ( $ET_{24h}$ )

##### 3.1.1 Determination of $Rn_{24h}$ values

To determine  $Rn_{24h}$  charts, an adaptation proposed by Ataide (2006) for the sinusoidal model estimator of the cycle of radiation balance for clear sky days, based in an approximation similar to the Lagourade and Brunet (1983) method, was adopted.

Looking forward for reliability and applicability in the generation of the  $Rn_{24h}$  charts from values of  $Rs_{\downarrow 24h}$ , a linear regression between the short wave balance and the daily radiation balance was performed, where the regression equation coefficients were determined as  $a = 0,9111$  and  $b = -23,918$ .

The coefficients obtained ( $a$  and  $b$ ) are next to the values found by Alados et al. (2003), whit values of  $a = 0,709$  and  $b = -25,4$  where values of global solar radiation ( $R_g$ ) and not short wave balance (BOC) were used in the linear regression, thus excluding the effect of the surface albedo in the calculation. Considering that values of  $R_g$  were determined in a standard meteorological station, installed on a grass field, with values of albedo varying between 20 and 25 %, the coefficients determined by the linear regression between values of BOC and  $Rn_{24h}$  tent to be in agreement with the values mentioned by Alados et al. (2003).

Thus, the radiation balance for the daily period ( $Rn_{24h}$ ) was ultimately determined for each pixel of the study scene by the equation:

$$Rn_{24h} = 0,9111 * (1 - \text{chart of albedo}) * Rs_{\downarrow 24h} - 23,918 \quad (11)$$

##### 3.1.2 Determination of the $ET_{24h}$ values

Based on charts of  $Rn$ ,  $G$ ,  $H$ ,  $LE$ ,  $T_s$  and  $\alpha$  and values of  $ET_{o24h}$  and  $ET_{o_{inst}}$ , estimated from data observed at Pesagro's meteorological station, four values of  $ET_{24h}$  were estimated for each scene studied:  $ET_{24h\_Classic}$  w/ $ET_{rF}$ ;  $ET_{24h\_Classic}$  w/ $Rn_{24h}$ ;  $ET_{24h\_H\_Pesagro}$  w/ $ET_{rF}$  and  $ET_{24h\_H\_Pesagro}$  w/ $Rn_{24h}$ .

Mean, maximum and minimum values obtained in charts of daily evapotranspiration ( $ET_{24h}$ ) estimated with the 'H\_Classic' proposition and expressed in  $\text{mm day}^{-1}$ , are showed in Table 1.

DJ	Mean		Maximum		Minimum	
	Rn 24h	ET <sub>r_F</sub>	Rn 24h	ET <sub>r_F</sub>	Rn 24h	ET <sub>r_F</sub>
218	3,42	4,25	6,51	12,69	0,0	0,0
227	2,88	2,89	6,89	7,64	0,0	0,0
230	3,13	3,19	6,99	7,76	0,0	0,0
241	3,25	2,98	7,39	7,48	0,0	-1,04
255	4,07	3,64	8,25	8,27	0,0	-0,10
285	4,82	4,17	9,63	9,82	0,0	-0,60
320	4,50	3,70	10,65	10,15	0,0	-1,10
339	5,25	4,52	10,75	10,37	0,0	-0,81
15	4,77	4,06	10,91	10,97	0,0	-2,17
36	4,65	4,16	10,12	10,34	0,0	-1,64
63	5,10	5,67	9,40	11,82	0,0	-0,37
102	4,06	3,67	7,75	8,23	0,0	-1,10
116	3,27	3,20	6,93	7,65	0,0	-2,22
139	2,78	2,71	5,94	6,62	0,0	-0,67
166	2,73	2,88	5,45	6,73	0,0	-0,43
186	2,16	2,47	5,48	6,93	0,0	-0,83
189	2,75	2,99	5,61	6,90	0,0	-0,13
190	3,09	2,71	7,23	7,08	0,0	-0,20
191	2,27	2,56	5,68	7,23	0,0	-1,23
200	2,02	2,28	5,51	7,11	0,0	-0,52
201	2,87	3,46	5,84	8,31	0,0	-0,02
205	3,36	4,03	5,84	8,31	1,05	1,07
208	2,54	3,09	6,09	8,26	0,0	-0,98
221	2,88	3,08	6,59	7,82	0,0	-1,25

Table 1. Statistical data of daily evapotranspiration charts (ET24h) of the study area using the ‘H\_Classic’ proposition w/ Rn24h and w/ ETr\_F, in mm day<sup>-1</sup>.

Average mean data showed in Table 1 are similar, with a slight superiority for the values estimated by the method using Rn24h for the ET estimative. Minimum values for ETr\_F have negative values. Tasumi et al. (2003), using SEBAL in Idaho, U.S.A., also observed negative values for ET and attributed such results to systematic errors caused by diverse parameterizations used during the process of energy balance estimation. Average mean, maximum and minimum values obtained in charts of daily evapotranspiration (ET24h) estimated with the “H\_Pesagro’ proposition, expressed in mm day<sup>-1</sup>, are showed in Table 2.

DJ	Mean		Maximum		Minimum	
	Rn 24h	ETr_F	Rn 24h	ETr_F	Rn 24h	ETr_F
218	4,45	5,34	6,51	13,38	2,39	2,18
227	4,65	4,61	6,89	7,71	1,87	1,53
230	4,83	4,86	6,99	7,75	0,78	0,60
241	5,84	5,26	7,44	7,53	4,44	3,45
255	6,00	5,30	8,26	8,28	3,78	2,79
285	7,29	6,21	9,75	9,94	5,17	3,82
320	7,31	5,84	10,69	10,39	4,64	3,14
339	7,01	5,99	10,81	10,70	2,17	1,40
15	7,92	6,51	10,96	11,02	2,60	1,48
36	8,12	7,01	10,23	10,84	5,79	4,24
63	6,69	7,35	9,46	12,07	3,90	3,60
102	5,41	4,85	7,75	8,23	0,80	0,50
116	4,62	4,56	6,95	7,65	0,0	-0,46
139	4,27	4,13	5,95	6,62	2,60	2,21
166	4,27	4,11	5,95	6,62	2,61	2,21
186	3,37	3,84	5,48	7,12	1,73	1,75
189	3,86	4,16	5,62	6,94	2,28	2,14
190	5,49	4,74	7,25	7,10	4,41	3,39
191	3,74	4,16	5,70	7,25	0,36	0,27
200	3,29	3,70	5,58	7,20	1,69	1,74
201	3,36	4,03	5,83	8,31	1,05	1,08
205	4,50	5,00	5,95	7,91	3,40	3,26
208	4,33	5,11	6,09	8,35	2,93	3,06
221	4,68	4,93	6,62	7,86	2,88	2,65

Table 2. Statistical data of daily evapotranspiration charts (ET 24h) of the study area using the ‘H\_Pesagro’ proposition w/ Rn 24hs and w/ ETr\_F, in mm day<sup>-1</sup>.

Average mean values of the same magnitude order and with a slight superiority to values estimated using Rn24h are observed in Table 2. In a general way, by the use of the ‘Classic’ proposal as well as by ‘Pesagro’ proposal, a higher amplitude of the estimated values is observed when using the method of ETr\_F.

Values of ET 24h<sub>SEBAL</sub>, observed in pixels where the micro-meteorological and meteorological stations were located (pixels from Pesagro, UFFRJ, Sugar-cane and Coconut), were correlated with values of ETo estimated by the equation of Penman-Monteith\_FAO (ETo PM\_FAO56) with data observed in Pesagro Station. Figures 5, 6, 7 and 8 show graphical representations of the regression analysis, the adjustment equation and the correlation coefficient (R<sup>2</sup>), obtained among the values estimated by SEBAL for all four methods used.

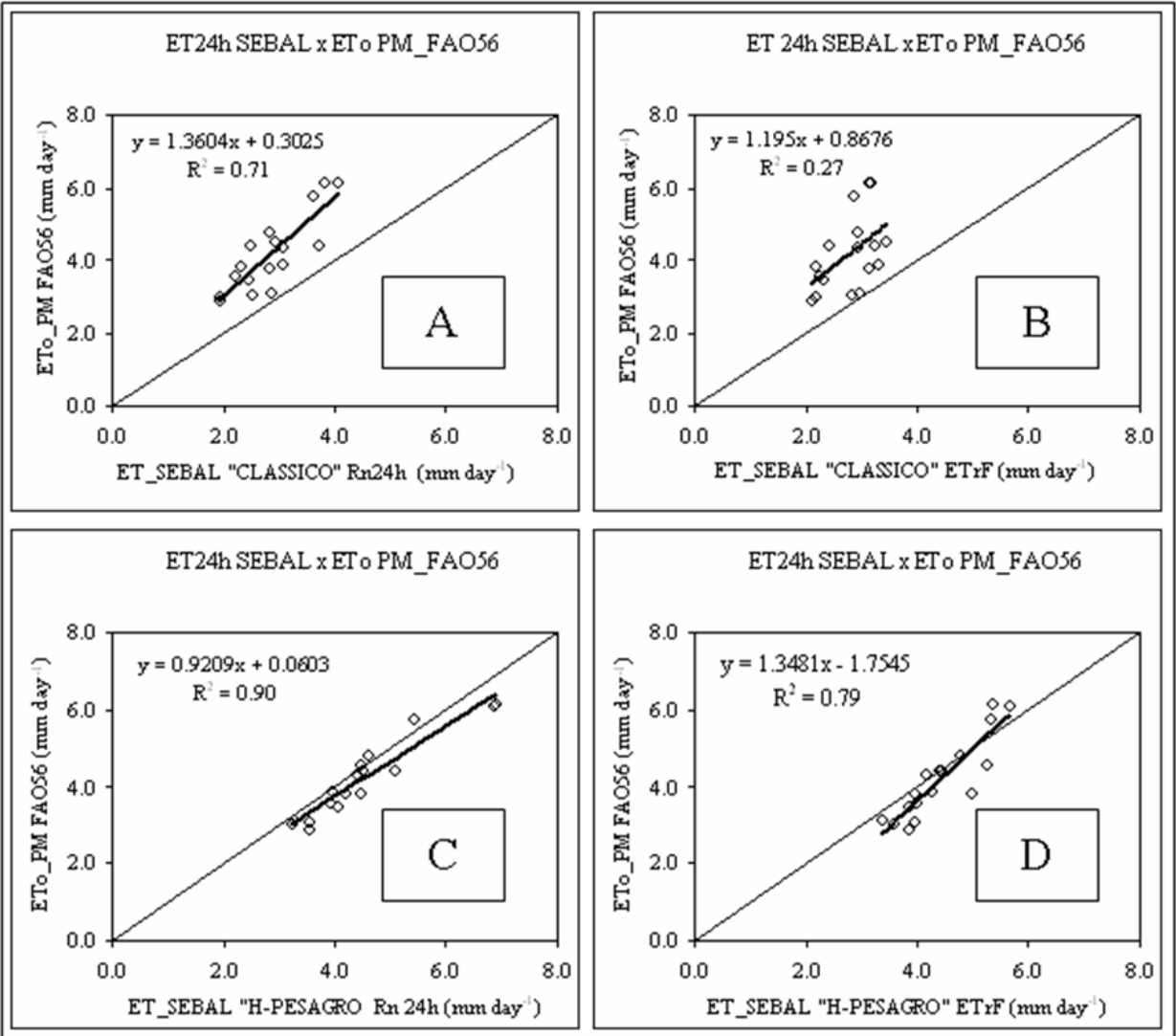


Fig. 5. Correlation between values of ET24h estimated with the method FAO (PM\_FAO56) with data collected at PESAGRO station and values of ET24h estimated by SEBAL with propositions "H\_Classic" w/Rn24h (A), "H\_Classic" w/ETr\_F (B), "H\_Pesagro" w/Rn24h (C) and "H\_Pesagro" w/ETr\_F (D) observed in pixel from Pesagro, expressed in mm day<sup>-1</sup>.

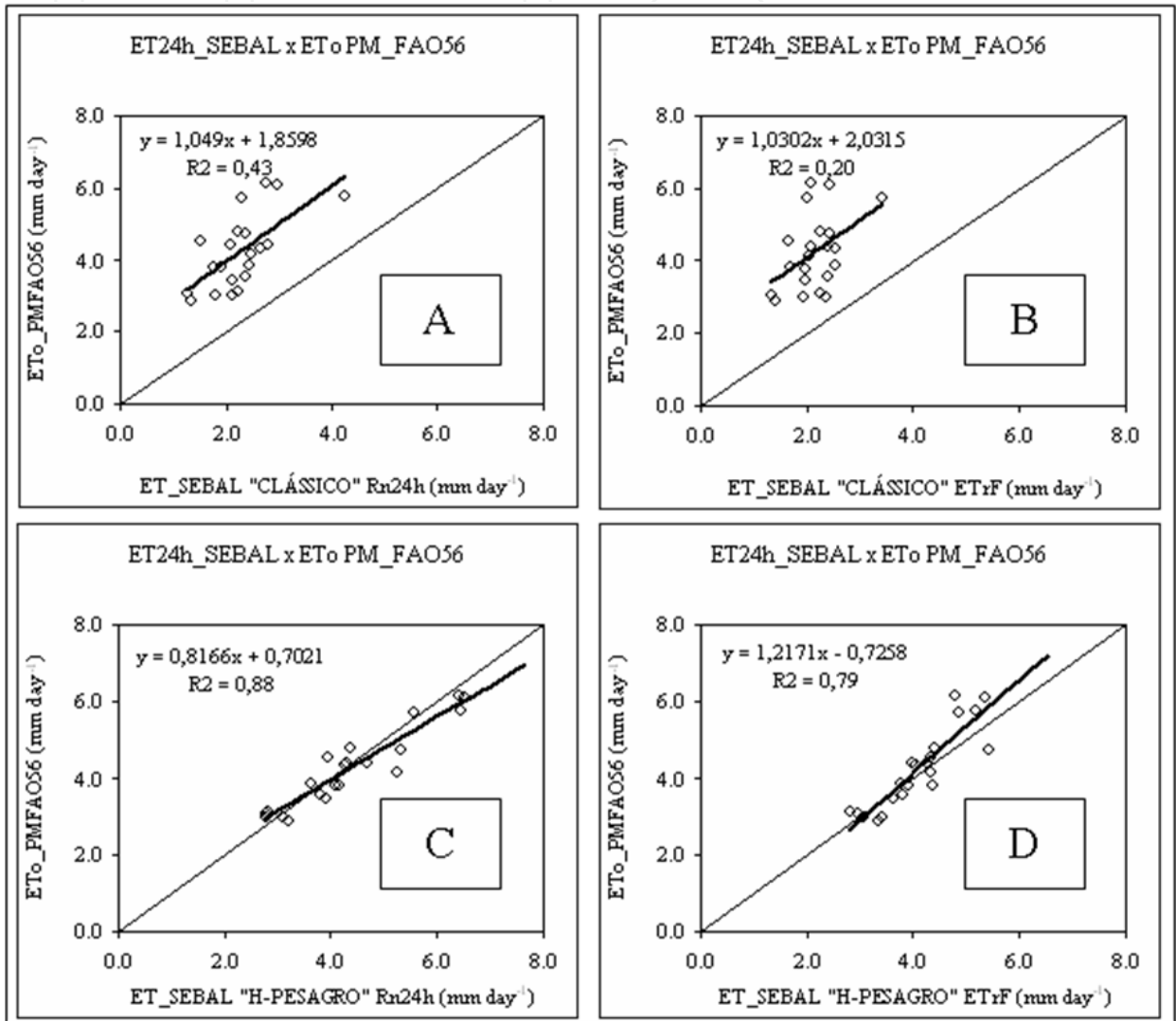


Fig. 6. Correlation between values of ET<sub>24h</sub> estimated with the method FAO (PM\_FAO56) with data collected in PESAGRO station and values of ET<sub>24h</sub> estimated by SEBAL with propositions "H\_Classic" w/Rn24h (A), "H\_Classic" w/ET<sub>r</sub>\_F (B), "H\_Pesagro" w/Rn24h (C) and "H\_Pesagro" w/ET<sub>r</sub>\_F (D) observed in pixel pixel from UFRRJ, expressed in mm day<sup>-1</sup>.

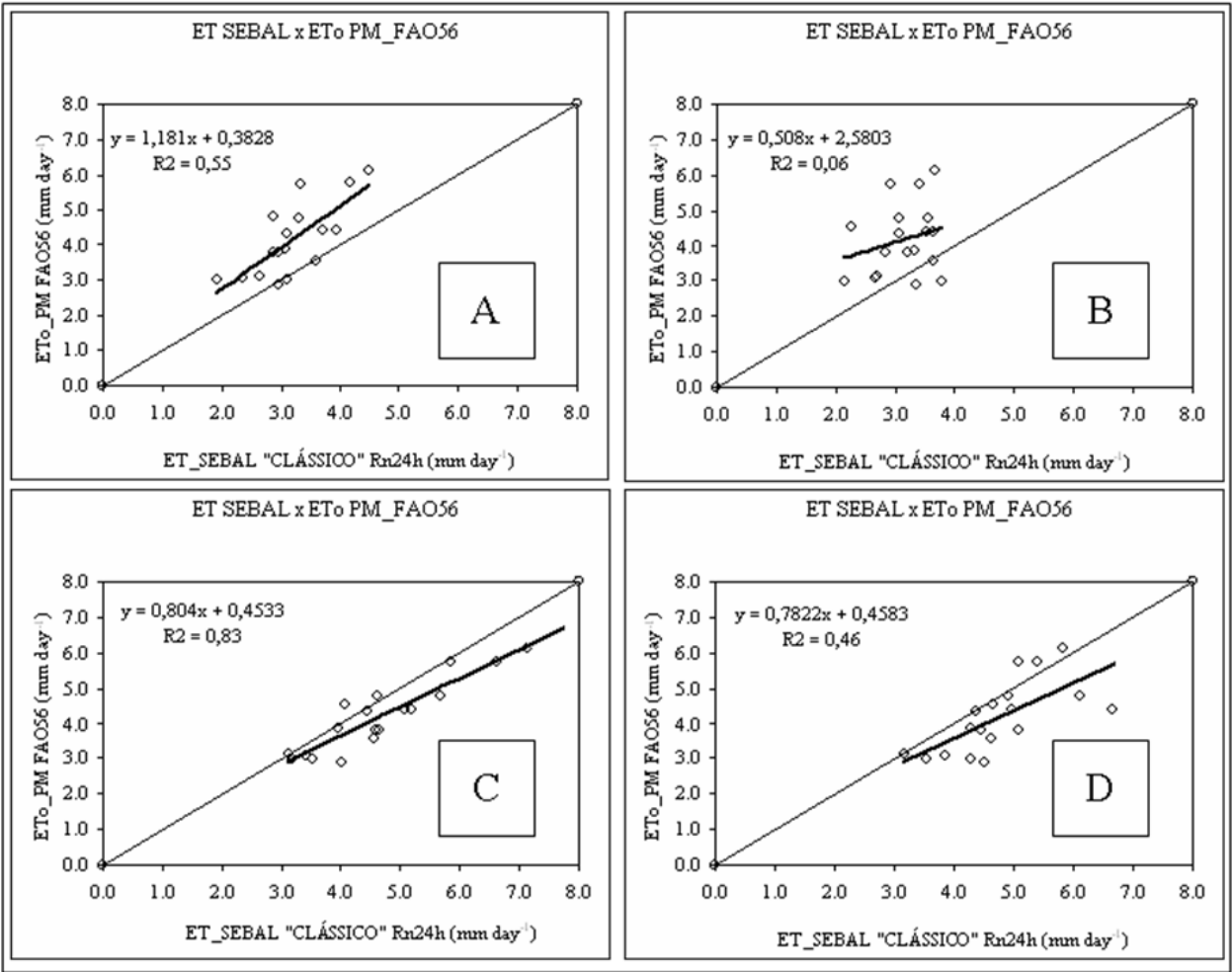


Fig. 7. Correlation between values of ET24h estimated by the method FAO (PM\_FAO56) with data collected from PESAGRO station and values of ET24h estimated by SEBAL with propositions “H\_Classic” w/Rn24h (A), “H\_Classic” w/ET<sub>Tr\_F</sub> (B), “H\_Pesagro” w/Rn24h (C) and “H\_Pesagro” w/ET<sub>Tr\_F</sub> (D) observed in pixel from Sugar-cane (SANTA CRUZ AGROINDUSTRY), expressed in mm day<sup>-1</sup>.

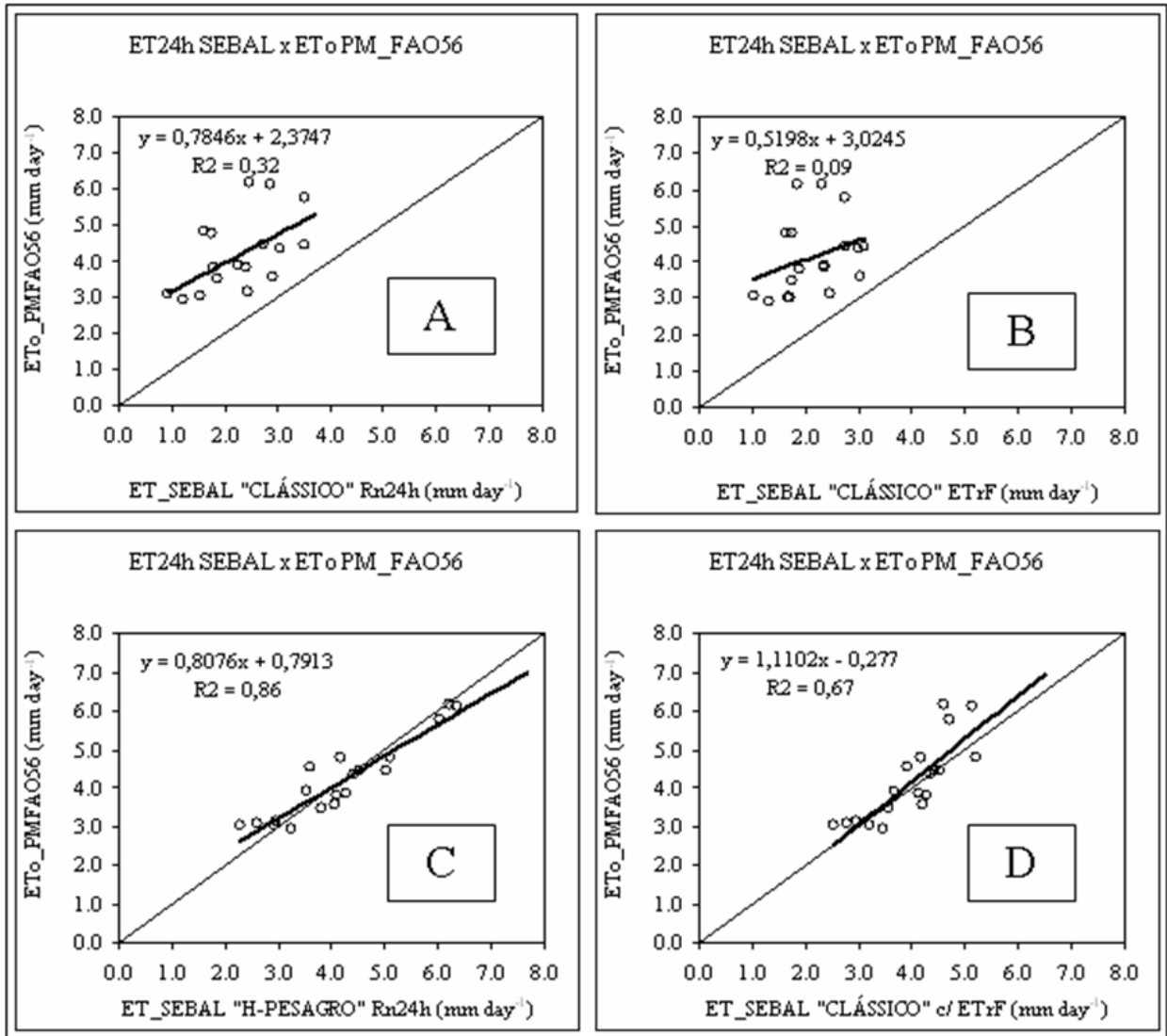


Fig. 8. Correlation between values of ET24h estimated by the method FAO (PM\_FAO56) with data collected from PESAGRO station and values of ET24h estimated by SEBAL with propositions “H\_Classic” w/Rn24h (A), “H\_Classic” w/ETr\_F (B), “H\_Pesagro” w/Rn24h (C) and “H\_Pesagro” w/ETr\_F (D) observed in pixel from Coconut (AGRICULTURE TAÍ) expressed in mm day<sup>-1</sup>.

Observing Figures 5, 6, 7, and 8, it is possible to conclude that the proposition ‘H\_Classic’ under estimated values projected by PM\_FAO56 method, showing better results for values estimated using Rn24h.

Proposition ‘H\_Pesagro’, although in a slight way, super estimated values of the ETo estimated with data from the meteorological station Pesagro, in all four control points, showing higher correction coefficients than the others with emphasis for the method using Rn24h.

Hafeez et al. (2002) applied SEBAL using MODIS images in Philippines and observed that the ET\_SEBAL super estimated in 13,5 % the values of ETo estimated by PM\_FAO56, justifying such behavior due to the spatial resolution of 1.000 m of the surface temperature chart (MOD11A1).

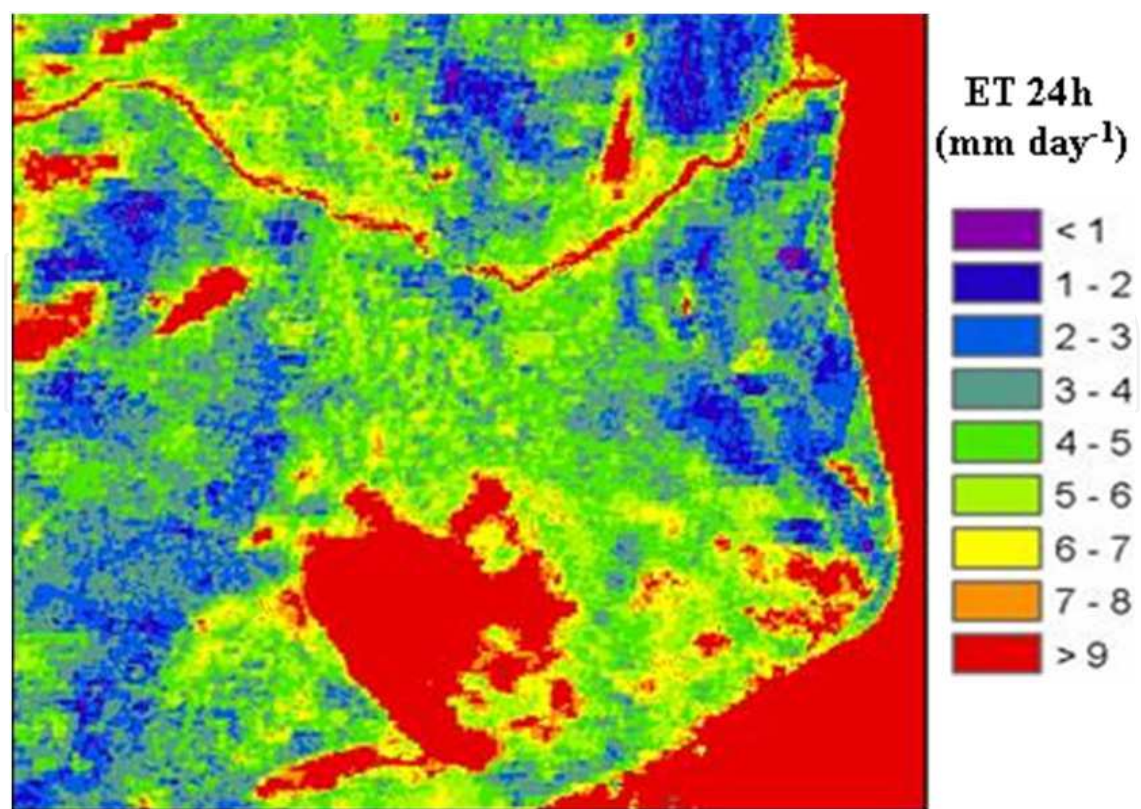


Fig. 9. Images of the daily evapotranspiration for the dry period in the Fluminense North Region, Rio de Janeiro State. DJ 2005218.

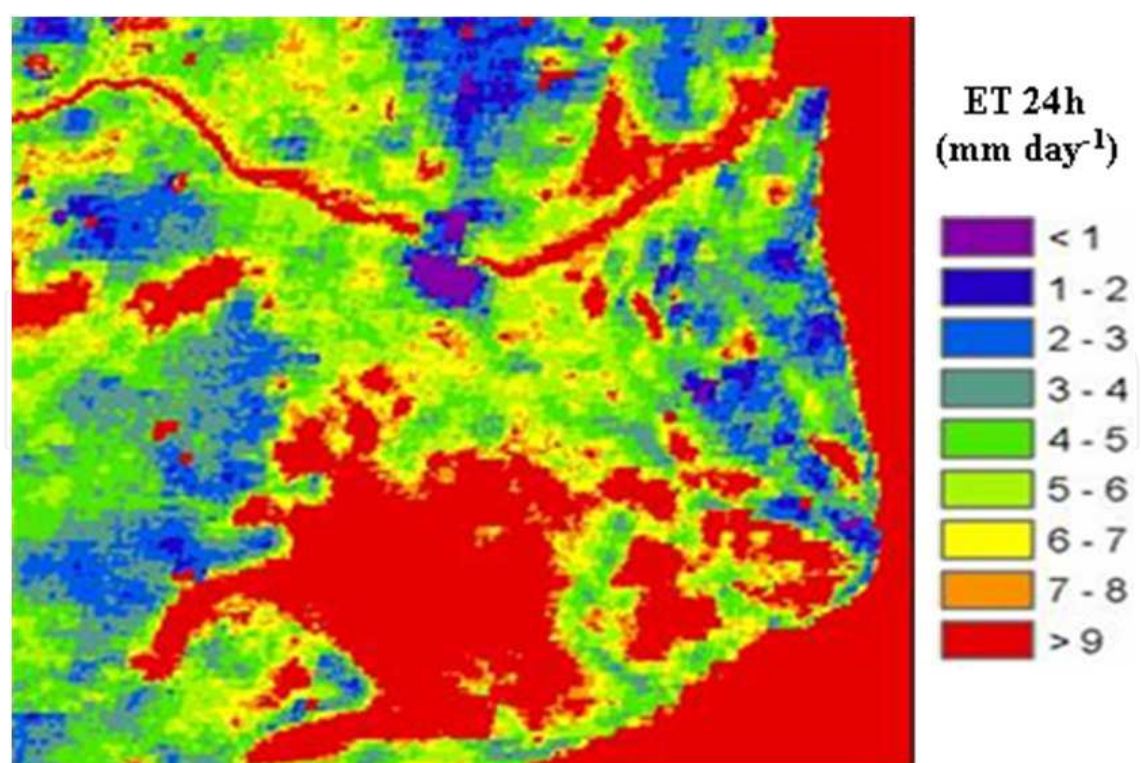


Fig. 10. Images of the daily evapotranspiration for the humid period in the Fluminense North Region, Rio de Janeiro State. DJ 2006015.

Allen et al. (2001), using images of LANDSAT in the basin of river Bear, North-East region of the U.S.A., observed that SEBAL showed a good precision for the estimation of ET, compared with weighing lysimeters, super estimating monthly mean values in 16% and 4 % for seasonal values.

Images of the daily evapotranspiration for the dry and humid periods in the Fluminense North Region, Rio de Janeiro State is showed in Figures 9 (DJ 2005218 ) and 10. (DJ 2006015).

#### 4. Conclusion

In accordance with the proposed objectives in this work, it is possible to conclude that in conditions de sub-humid climate: For the estimative of sensible heath flux, the use of proposition 'H\_Pesagro' resulted more efficient than 'H\_Classic'; The method that uses values of mean radiation balance integrated in 24 hours (Rn24h) is more consistent than the method that uses the reference evaporative fraction (ET<sub>r\_F</sub>) for the conversion of instantaneous evapotranspiration values (ET<sub>inst</sub>) in daily values (ET<sub>24h</sub>).

#### 5. Acknowledgements

The authors are grateful for the National Counsel for Scientific and Technological Development – CNPq and the Coordenação de Aperfeiçoamento de Pessoal de Nível Superior – CAPES, for the financial support and logistics that made this study possible.

#### 6. References

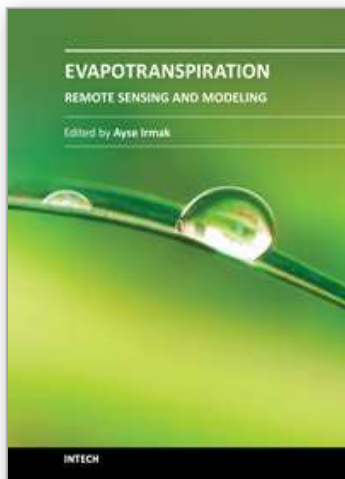
- Alados, C.L.; Pueyo, Y.; Giner, M.L.; Navarro, T.; Escos, J.; Barroso, F.; Cabezudo, B.; Emlen, G.M., 2003. Quantitative characterization of the regressive ecological succession by fractal analysis of plant spatial patterns. *Ecological Modell.* v.163, p.1-17.
- Allen, R. G.; Pereira, L. S.; Raes, D.; Smith, M., 1998. Crop evapotranspiration – Guidelines for computing crop water requeriments. FAO Irrigation and Drainage Paper 56, Rome, Italy, 318 p.
- Allen, R.G.; Tasumi, M.; Trezza, R.; Bastiaanssen, W.G.M., 2002. SEBAL - Surface Energy Balance Algorithms for Land. Advanced training and users manual, Version 1.0. University of Idaho, EUA. 97 p.
- Ataíde, K.R.P., 2006. Determinação do saldo de radiação e radiação solar global com produtos do sensor MODIS Terra e Aqua. Tese (Mestrado em Meteorologia) - Campina Grande, PB - Universidade Federal de Campina Grande - UFCG, 88p.
- Azevedo, H.J.; Silva Neto, R.; Carvalho, A. M.; Viana, J.L.; Mansur, A.F.U., 2002. Uma análise da cadeia produtiva da cana-de-açúcar na Região Norte Fluminense. Observatório sócio-econômico da Região Norte Fluminense – Boletim Técnico nº 6, 51p.
- Bastiaanssen, W.G.M., 1995. Regionalization of surface flux densities and moisture indicators in composite terrain. Ph,D Thesis, Wageningen Agricultural University, Wageningen, The Netherlands. 273p.
- Bastiaanssen, W.G.M.; Pelgrum, H.; Wang, J.; Ma, Y.; Moreno, J.; Roerink, G. J.; van der Val, T., 1998. A remote sensing surface energy balance algorithm for land (SEBAL):Part 2 validation, *Journal of Hidrology*, v, 212-213: 213-229.

- Frota, P.C.E., 1978. Estudo do calor sensível e latente no interior de uma cultura de milho (*Zea mays* L.), Dissertação (Mestrado em Agrometeorologia), Piracicaba, SP, Universidade Luiz de Queiroz - ESALQ/USP, 75p.
- Gomes, M.C.R., 1999. Efeito da irrigação suplementar na produtividade da cana-de-açúcar em Campos dos Goytacazes, RJ. Dissertação (Mestrado em Produção Vegetal) - Campos dos Goytacazes - RJ, Universidade Estadual do Norte Fluminense - UENF, 51p.
- Hafeez, M.M.; Chemin, Y.; Van de Giesen, N.; Bouman, B.A.M., 2002. Field evapotranspiration estimation in Central Luzón, Philippines, using different sensors: Landsat 7 ETM+, Terra Modis and Aster. Symposium on Geospatial Theory, Processing and Applications. Ottawa-Canadian. 7 p.
- Ide, B. Y.; Oliveira, M.A. de, 1986. Efeito do clima na produção da cana-de-açúcar. In: Seminário de Tecnologia Agrônômica, 3. Piracicaba, SP. Anais.... São Paulo: COPERSUCAR, p.573-583.
- Lagouarde, J.P.; Brunet, Y., 1983. A simple model for estimating the daily upward long wave surface radiation flux from NOAA/AVHRR data. International Journal of Remote Sensing. 14(5):907-925.
- Land Processes Distributed Active Archive Center - LP-DACC Available online: <http://edcimswww.cr.usgs.gov/pub/imswelcome/> (Accessed on 15 April/2005).
- Magalhães, A. C. N. 1987. Ecofisiologia da cana-de-açúcar: aspectos do metabolismo do carbono na planta. In: Castro, P.R.C.; Ferreira, S.O.; Yamada, T. (Ed.). Ecofisiologia da Produção Agrícola. Piracicaba, SP: Potafós, p. 113-118.
- Moran, M. S.; Jackson, R. D.; Raymond L.; Gay, L.; Slater, P., 1999. Mapping surface energy balance components by combining Landsat Thematic Mapper and ground-based meteorological data. Remote Sensing of Environment. n.30:77-87.
- Morgado, I.F., 2009. Agroindústria Sucroalcooleira do Estado do Rio de Janeiro. Universidade Cândido Mendes - UCAM. Available online: [http://www.infoagro.ucam-campos.br/agro\\_in\\_rio.htm](http://www.infoagro.ucam-campos.br/agro_in_rio.htm). (Accessed on 25 June/2010).
- Paiva, C.M.; Liu, W.T.H.; Franca, G.B.; Filho, O.C. R., 2004. Estimativa das componentes do balanço de energia via satélite através do modelo SEBAL. XIII Congresso Brasileiro de Meteorologia, Fortaleza, CE. Anais.
- Roerink, G.J.; Bastiaanssen, W.G.M.; Chambouleyron, J.; Menenti, M., 1997. Relating crop water consumption to irrigation water supply to remote sensing. Water Resources Management. 11: 445-465.
- Secretaria Estadual de Agricultura, Pesca e Desenvolvimento do Interior - SEAAPI, RJ (2006). Available online: [www.seaapi.rj.gov.br/frutificar](http://www.seaapi.rj.gov.br/frutificar). (Accessed on 15 November/ 2006).
- Silva, B.B.; Lopes, G.M.; Azevedo, P.V., 2005. Balanço de radiação em áreas irrigadas utilizando imagens Landsat 5 -TM. Revista Brasileira de Meteorologia. V.20 (2): 243-252.
- Tasumi, M., 2003. Progress in operational estimation of regional evapotranspiration using satellite imagery. PhD Dissertation. Idaho State University. Idaho. USA. 379 p.
- Teixeira, A. H. C., 2008. Measurements and modelling of evapotranspiration to assess agricultural water productivity in basins with changing land use patterns - a case study in the São Francisco River basin, Brazil. PhD Dissertation. Wageningen University.. Nederland. 239 p.

- Timmermans, W.J.; Meijerink, A.M.J., 1999. Remotely sensed actual evapotranspiration: implications for groundwater management in Botswana. *Journal of Applied Geohydrology*. 1:222-233.
- Trezza, R., 2002. Evapotranspiration using a satellite-based energy balance with standardized ground control. PhD Dissertation. Utah State University. Logan. USA. 247p.

IntechOpen

IntechOpen



## **Evapotranspiration - Remote Sensing and Modeling**

Edited by Dr. Ayse Irmak

ISBN 978-953-307-808-3

Hard cover, 514 pages

**Publisher** InTech

**Published online** 18, January, 2012

**Published in print edition** January, 2012

This edition of Evapotranspiration - Remote Sensing and Modeling contains 23 chapters related to the modeling and simulation of evapotranspiration (ET) and remote sensing-based energy balance determination of ET. These areas are at the forefront of technologies that quantify the highly spatial ET from the Earth's surface. The topics describe mechanics of ET simulation from partially vegetated surfaces and stomatal conductance behavior of natural and agricultural ecosystems. Estimation methods that use weather based methods, soil water balance, the Complementary Relationship, the Hargreaves and other temperature-radiation based methods, and Fuzzy-Probabilistic calculations are described. A critical review describes methods used in hydrological models. Applications describe ET patterns in alpine catchments, under water shortage, for irrigated systems, under climate change, and for grasslands and pastures. Remote sensing based approaches include Landsat and MODIS satellite-based energy balance, and the common process models SEBAL, METRIC and S-SEBS. Recommended guidelines for applying operational satellite-based energy balance models and for overcoming common challenges are made.

### **How to reference**

In order to correctly reference this scholarly work, feel free to copy and paste the following:

José Carlos Mendonça, Elias Fernandes de Sousa, Romísio Geraldo Bouhid André, Bernardo Barbosa da Silva and Nelson de Jesus Ferreira (2012). Assessment of Evapotranspiration in North Fluminense Region, Brazil, Using Modis Products and Sebal Algorithm, Evapotranspiration - Remote Sensing and Modeling, Dr. Ayse Irmak (Ed.), ISBN: 978-953-307-808-3, InTech, Available from:  
<http://www.intechopen.com/books/evapotranspiration-remote-sensing-and-modeling/assessment-of-evapotranspiration-in-north-fluminense-region-brazil-using-modis-products-and-sebal-al>

**INTech**  
open science | open minds

### **InTech Europe**

University Campus STeP Ri  
Slavka Krautzeka 83/A  
51000 Rijeka, Croatia  
Phone: +385 (51) 770 447  
Fax: +385 (51) 686 166  
[www.intechopen.com](http://www.intechopen.com)

### **InTech China**

Unit 405, Office Block, Hotel Equatorial Shanghai  
No.65, Yan An Road (West), Shanghai, 200040, China  
中国上海市延安西路65号上海国际贵都大饭店办公楼405单元  
Phone: +86-21-62489820  
Fax: +86-21-62489821

© 2012 The Author(s). Licensee IntechOpen. This is an open access article distributed under the terms of the [Creative Commons Attribution 3.0 License](#), which permits unrestricted use, distribution, and reproduction in any medium, provided the original work is properly cited.

IntechOpen

IntechOpen